

Supercell and cluster density functional calculations of the thermal stability of the divacancy in germanium

C. Janke* and R. Jones

School of Physics, University of Exeter, Stocker Road, Exeter EX4 4QL, United Kingdom

S. Öberg

Department of Mathematics, Luleå University of Technology, Luleå S-97187, Sweden

P. R. Briddon

School of Natural Sciences, University of Newcastle upon Tyne, Newcastle upon Tyne, NE1 7RU, United Kingdom

(Received 18 September 2006; revised manuscript received 16 January 2007; published 16 May 2007)

Large vacancy clusters, or voids, formed during crystal growth have been reported in Ge. The divacancy is a precursor to such clusters, and is believed to be stable up to 150 or 180 °C. It is also believed to form in Ge irradiated at room temperature where single vacancies are mobile. Density functional theory (DFT) cluster calculations have been performed to calculate the energy barriers for migration and dissociation of the divacancy. We find that the binding energy in the neutral charge state is ~ 1.5 eV and increases for negatively charged states. The migration energies were found to vary from 1.0 to 1.3 eV from the singly positive to the doubly negative charge states. These results line up well with an estimate of a migration barrier of 1.0 eV for the divacancy from experimental data. Therefore, we conclude that the divacancy in germanium will anneal by migration to trapping centers.

DOI: [10.1103/PhysRevB.75.195208](https://doi.org/10.1103/PhysRevB.75.195208)

PACS number(s): 61.72.Bb, 61.72.Ji, 61.72.Cc, 61.72.-y

I. INTRODUCTION

Vacancies (V) are one of the most basic defects in a crystalline material. In germanium, they are believed to play an especially important role, arising from their low formation energy when compared with the self-interstitial.^{1,2} There have been a number of previous studies on the single vacancy, dealing with their diffusivity,^{1,3,4} energy levels,^{2,5-7} and atomic structure,^{2,5,7-10} and the vacancy has been suggested as the primary mediating species for self-diffusion¹¹ and diffusion of some impurities.¹²

With the high mobility and low formation energy of vacancies, it would not be surprising to find vacancy clusters forming easily in germanium. Indeed, large voids have been observed following growth of germanium crystals, with diameters ranging from hundreds of nanometers up to tens of micrometers.^{13,14} Such voids would severely damage a device if they form within its active region. The first stage to the formation of such voids would be the formation of divacancies, and these defects will be the focus of this paper.

Although the divacancy (V_2) has been studied previously using both *ab initio* methods and experiments, its properties and identification are still the object of some controversy. Structurally, they were shown to have similar properties to the silicon case, although with much weaker Jahn-Teller distortions and energies.¹⁰ In fact, the calculated distortion magnitudes and types found in cluster calculations are sensitive to the lattice parameter that was employed to generate the cluster.^{10,15} Energy levels have also been calculated from *ab initio* methods, with a donor level found to lie at $E_V + 0.03$ eV and two acceptor levels at $E_V + 0.3$ eV and $E_C - 0.4$ eV.¹⁵ Two deep-level transient spectroscopy studies also report results for the divacancy. Poulin and Bourgoin¹⁶ and Mooney *et al.*¹⁷ reported a pair of electron traps at E_C

-0.35 eV and $E_C - 0.32$ eV, which anneal at 150 °C and are attributed to the divacancy. However, Fage-Pedersen *et al.*¹⁸ linked the divacancy to a shallower electron trap at $E_C - 0.29$ eV which anneals at 180 °C. Infrared absorption studies by Whitehouse¹⁹ show an absorption band which is attributed to an internal electronic transition at the divacancy. This band anneals out at 200 K, i.e., significantly below room temperature, and its assignment has been questioned by Morrison and Newman²⁰

There are two ways in which V_2 could anneal. First, it might dissociate into highly mobile vacancies. This would be expected to occur at the rate $\nu \exp(-W/kT)$, where ν is an atomic jump frequency taken to be 10^{13} s⁻¹, and hence the activation energy should be $W \sim 1.3$ eV in order that V_2 anneals around 150 to 180 °C after 15 min. Second, if V_2 anneals by migration to a trap, the preexponential factor ν would be very much smaller as the defect must make many migratory jumps before reaching a trap. Assuming a trapping center density of $\sim 10^{18}$ cm⁻³, the preexponential factor would be decreased by a factor of about 10^4 . This implies that the energy barrier for diffusion of V_2 would be ~ 1.0 eV for V_2 to anneal around 150 to 180 °C.

It is interesting to compare the annealing of V_2 in Ge with that of Si.²¹ The energy barrier for reorientation of V_2 in Si is 1.3 eV which is a process involving a single lattice jump. The dissociation barrier is at least 1.9 eV. Thus, in oxygen-rich Si, the defect anneals around 300 °C through a migration mechanism with a barrier of 1.3 eV. It is the principal aim of this paper to determine the migration and dissociation barriers for V_2 .

Ab initio calculations have in the past been performed using one of two methods to treat the boundary conditions. The supercell method uses periodic boundary conditions, forming an infinite superlattice as an approximation to the

bulk. The cluster method models instead a nanoparticle, with the boundaries being surfaces to vacuum. Further refinement of the cluster method usually involves passivating the dangling bonds at the surface with hydrogen atoms, and holding the surface hydrogen and semiconductor atoms fixed while relaxing the bulk of the cluster. Both methods should tend to true bulk values in the limit of infinite size.

Both cluster and supercell methods have problems associated with them, and this study used both methods for different properties. The cluster method cannot be used to calculate formation energies, and calculations within the cluster method require significantly more computing resources at least for large clusters. Supercell calculations on the other hand suffer from a severe underestimation of the band gap due to the approximation to the exchange correlation energy employed within the local-density approximation (LDA) of density functional theory (DFT). This underestimation is catastrophic for Ge where the experimental band gap is small and the dispersion of defect energy levels, due to defect-defect interaction in the superlattice, is large with the result that the defect-related levels cross into the valence or conduction band and lead to serious errors. This is especially the case when dealing with charged defects where additional electrons are not localized on the defect.²² It will be seen below in Sec. III B that the small band gap causes defect energy levels to reside within the valence band at \mathbf{k} points used to sample the Brillouin zone. Cluster calculations were therefore used for the remainder of the study.

In Sec. II, the theoretical method employed shall be discussed, and the results of these calculations shall be presented in Sec. III. Section IV contains a summary of the results and discussion of the conclusions that can be drawn from them, while finally Sec. V contains our concluding remarks.

II. METHOD

Calculations were performed using a local-density functional code AIMPRO,²³ and the divacancy was embedded in hydrogen-terminated clusters and periodic supercells of Ge atoms. Initially, supercells were the focus of the work, but for reasons explained in Sec. III B the work was expanded to use the cluster method as well. A Padé parametrization²⁴ of the exchange-correlation functional as proposed by Perdew and Wang²⁵ was used, and the core electrons were accounted for by the pseudopotentials of Hartwigsen *et al.*²⁶

A real-space Gaussian contracted basis set consisting of (s, p, d) orbitals with $(4, 4, 1)$ distinct exponents, respectively, and optimized for bulk Ge was used to expand the Kohn-Sham states of the germanium. The orbitals of the hydrogen surface atoms were expanded using contracted basis sets with four s and one p exponents.

The supercells used were cubic shaped and consisted of 216 atoms for the perfect crystal, and the Brillouin zone was sampled using a Monkhorst-Pack sampling scheme of eight points (MP-2³).²⁷

The Ge clusters used were atom centered, near spherical in shape, and saturated with hydrogen atoms at the surface to passivate dangling bonds. The perfect clusters then com-

prised 329 Ge and 172 H atoms. They were generated using the experimental lattice parameter (5.657 Å).²⁸

Three types of cluster were investigated. In the first, the surface hydrogen-germanium bonds were strained to reproduce the experimental band gap.²² The defect was then introduced and the cluster was relaxed, holding the terminating hydrogen and surface germanium atoms fixed. In the second, the hydrogen atoms were first relaxed while holding all germanium atoms fixed in their positions determined by the lattice parameter. The defect was then introduced and all the bulk Ge atoms were allowed to relax while the surface H and Ge atoms were fixed. In the third, all atoms were allowed to relax. In the first two methods, the results can be sensitive to the lattice parameter used to generate the cluster, but the effect of this is very much weaker in the third method.

In both clusters and supercells, a divacancy was introduced by removing two atoms, and the surrounding atoms displaced to break the symmetry and facilitate rebonding of dangling bonds. Calculations were also performed with two remote vacancies separated by four neighboring sites, as it has been shown that for silicon, vacancies at this distance are effectively separate.²⁹ In the supercell calculations, the binding energy was also calculated from the formation energies of V and V_2 . Migration energies and paths were calculated using the improved tangent nudged elastic band method (NEB).³⁰ In this method, initial and final configurations are linearly interpolated to give a chain of intermediate structures or images. The images are then relaxed, with consecutive images interacting via virtual “elastic bands.” Relaxation is continued until the forces on the atoms in each image, including the elastic band forces, vanish. Similar methods have been used in the past to study various defects in germanium including divacancies,¹⁵ single vacancies,^{1,7} vacancy-oxygen complexes,³¹ vacancy-donor complexes,³² and oxygen interstitial structures.³³

III. RESULTS

A. Supercell calculations

1. Binding energies

Binding energies were calculated by two methods in the supercell calculations. The first method involves calculating the total energy of the perfect supercell, and the supercell with one and two vacancies within it. From this, the formation energies of the monovacancy and divacancy can be calculated from

$$E_f(MV) = E(N - M) - \frac{N - M}{N} E(N), \quad (1)$$

where $E_f(MV)$ is the formation energy of an M -vacancy cluster, N is the number of atoms in the perfect system, and $E(X)$ is the energy of the system with X Ge atoms in it. By comparing the formation energies of the monovacancy and divacancy, the binding energy can be obtained. This method gave 0.6 eV for the binding energy. The second method involves separating the vacancies within a common supercell and directly comparing the energies of the two systems. We find, for vacancies separated by four neighbors, the binding

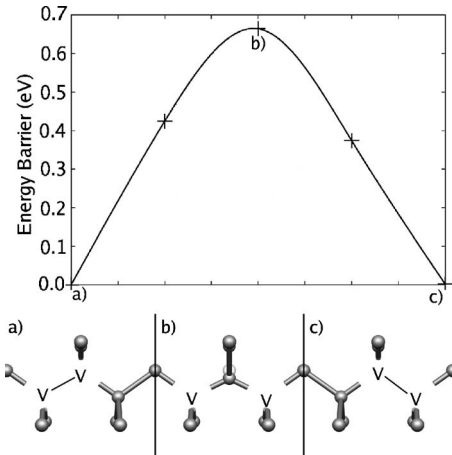


FIG. 1. Top: diffusion barrier shape for the divacancy diffusion in the supercell. Bottom: atomic configuration of (a) the initial structure, (b) the saddle point, and (c) the final structure. The transparent atom in the saddle-point configuration indicates the undisturbed crystal position as an aid to the reader.

energy to be 0.7 eV and very close to that found by the first method. This shows that the vacancies are essentially free at this separation, around 8 Å. It was also attempted to use this method to study charged defects, but only negligible changes in formation and binding energies were observed for any of the charge states examined. This was attributed to the small LDA band gap found in Ge. Charging the supercell then leads to occupation of the host bands instead of those of the defect.

2. Migration energies

Migration energies were calculated by the NEB method. The end points used were relaxed divacancies separated by one *atomic jump*, so a single Ge atom traverses the divacancy in each diffusion step. Figure 1 displays the shape of the migration barrier and the saddle-point configuration.

The saddle point was seen to be very close to the configuration with two vacancies at second-neighbor sites in the crystal. The energy barrier was found to be at 0.7 eV.

B. Band-structure analysis

In order to check the validity of the supercell results, the energy levels of a supercell containing V_2 were calculated and are plotted in Fig. 2 along with the valence and conduction bands of a bulk supercell. The levels introduced by the divacancy into the band gap are seen to cross into the valence band for a range of \mathbf{k} values along the symmetry directions sampled. This includes the Γ point and one of the MP-2³ sampling points examined in this plot. This is almost certainly an erroneous result due to the underestimation of the band gap within the supercell methodology, which in turn stems from the LDA treatment of the exchange-correlation energy and explains the insensitivity of the migration energy found above to the charge state. It also brings the results of the migration energy of neutral V_2 given above into question, as at the saddle-point levels will incorrectly cross into the

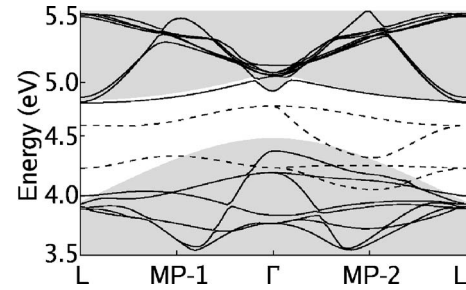


FIG. 2. Band structure for the divacancy (lines) between the gamma point and two L points with the valence and conduction bands of the perfect crystal presented for comparison (shaded regions). Included in these directions are two of the sampling points used in the MP-2³ scheme. As can be seen, the conduction-band energy levels are barely affected by the introduction of the divacancy to the system, while the valence-band energy levels are strongly distorted. Defect-related states (dashed lines) are seen to cross into the valence band at the Γ point and the second of the MP-2³ sampling points shown.

valence band. We therefore turned to cluster calculations for the remainder of the study.

C. Cluster calculations

1. Binding energies

Due to the confined nature of a cluster calculation and the existence of a hydrogenated surface, it is impossible to calculate binding energies using isolated vacancies in the manner described in Sec. III A 1. Instead, we must use the alternative method, separating the vacancies within the same cluster. When the surface of the cluster is confined, the method will give higher binding energies than would be the case without the defect-surface interaction, as the rigid surface restricts relaxation of the atoms around the vacancies and thus the separated vacancies, which are closer to the surface, are in a less relaxed configuration. To avoid spurious charge transfer between the vacancies, only evenly charged states could be calculated. Results are given in Table I for binding energies calculated in all three cluster types.

TABLE I. Binding (E_B), migration (E_M), and symmetry constrained saddle point (E_{sbsp}) energies, in eV of the divacancy found in 501 atom clusters with strained surface bonds, relaxed surface bonds, and fully relaxed surfaces for various charge states.

| Surface | Charge | E_B | E_M | E_{sbsp} |
|-----------------|--------|-------|-------|-------------------|
| Strained | + | | | 1.0 |
| | 0 | 1.5 | 1.1 | 1.1 |
| | - | | 1.2 | 1.2 |
| Relaxed bonds | = | 1.6 | 1.3 | 1.3 |
| | 0 | 1.7 | | 1.1 |
| Relaxed surface | = | 1.8 | | 1.3 |
| | 0 | 1.7 | | 1.1 |

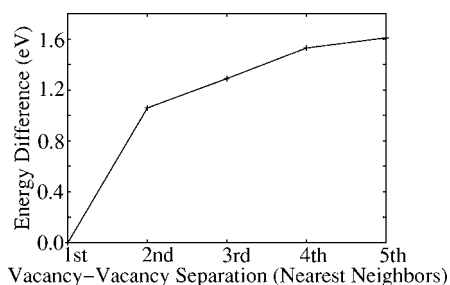


FIG. 3. Figure showing the increase in energy upon separating the divacancy from a first nearest-neighbor configuration out to a fifth neighbor configuration.

The binding energies show an increase in stability with the more negatively charged states and are also notably higher than the supercell case. Results calculated in clusters with relaxed surface bonds and fully relaxed surfaces are also shown, with the binding energy seen to increase when the surface bonds are relaxed. Charging the cluster with relaxed surface bonds yielded the same shifts in energy barriers as for the cluster with strained surface bonds.

In order to check the applicability of this method to germanium cluster calculations, convergence with respect to intervacancy distance was calculated for clusters with strained surface bonds, and the results are summarized in Fig. 3. In the fourth nearest-neighbor configuration, where the vacancies are considered to be separated, each vacancy is at a third neighbor site from a surface germanium atom. It is therefore not expected for the graph to completely level out, and the energy difference between the fourth and fifth neighbor configurations is considered small, and is likely dominated by vacancy-surface interactions. Furthermore, the difference between these energies allows an estimate of the contribution of surface interaction on the binding energy to be made, suggesting an overestimate of around 0.2 eV from this source.

2. Migration energies

Migration energies were again calculated using the NEB method, with the migration occurring symmetrically about the center of the cluster. The saddle point was again shown to be close to the second nearest-neighbor configuration having C_{2v} symmetry. Symmetry-constrained relaxations were performed with this configuration, and the energy difference from the bound divacancy is reported in Table I (E_{scsp}) along with the migration energies. As can be seen, the barrier calculated by the NEB method and those calculated by this relaxation are in excellent agreement, and the latter migration barriers were calculated solely by this method. Comparing the results calculated for different surface conditions reveal a negligible change in the migration barrier of the order of ± 0.03 eV across all charge states tested.

Similarly to the binding energies, the migration energies show an increase as the charge state becomes more negative.

D. Atomic structure

The divacancy is seen in both supercell and cluster calculations to be unstable against Jahn-Teller (JT) distortions.

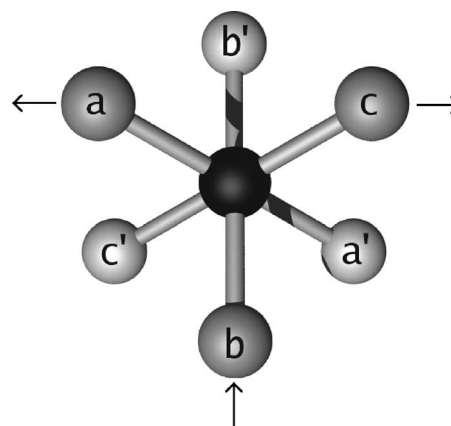


FIG. 4. Diagram showing an end-on view of an undistorted divacancy. The vacancy sites (black) are surrounded by three Ge atoms at each end (light and dark gray, respectively). The JT distortions observed in the divacancy preserve the reflection symmetry plane containing the two vacant sites and the atoms b and b' . Resonant bonding occurs when $ab=bc < ac$, as indicated by arrows in the diagram.

These are spontaneous lowering of the symmetry of the system accompanied by a lowering in the energy as dangling bonds from the Ge atoms surrounding the divacancy link up and rebond. As shown in Fig. 4, the JT distortions maintain the reflection symmetry with a plane of reflection through the b and b' atoms. If, as shown in Fig. 4, the atoms move such that $ab=bc < ac$ (and likewise $a'b'=b'c' < a'c'$), the distortion forms a resonant bonding (RB) structure, as there is a resonant reconstructed bond between the three atoms. If instead, the atoms move in the opposite sense, such that $ab=bc > ac$, there is instead a pairing bond between atoms a and c , and this distortion forms a pairing structure.

As is shown in Table II, the neutral divacancy is seen to relax into a RB configuration in supercell and most cluster calculations. In charged cluster calculations and neutral cal-

TABLE II. Interatomic distances for atoms surrounding the divacancy, in angstroms, and percentages of unrelaxed values, using the labeling scheme from Fig. 4. Results are presented for both supercell and cluster calculations. Within the cluster methodology, results for different charge states and surface conditions are presented.

| Method | Charge | ab | ac | aa' |
|-------------------------------|--------|------------|------------|------------|
| Supercell | 0 | 3.19 (81%) | 3.33 (84%) | 5.40 (89%) |
| Cluster with strained surface | + | 3.77 (95%) | 3.77 (95%) | 6.00 (98%) |
| | 0 | 3.60 (90%) | 3.77 (95%) | 5.86 (95%) |
| | - | 3.60 (90%) | 3.60 (90%) | 5.78 (94%) |
| Relaxed bonds | = | 3.53 (88%) | 3.53 (88%) | 5.67 (92%) |
| | 0 | 3.73 (94%) | 3.73 (94%) | 5.93 (96%) |
| Fully relaxed | = | 3.53 (89%) | 3.53 (89%) | 5.66 (92%) |
| | 0 | 3.31 (83%) | 3.75 (94%) | 5.70 (93%) |

culations with relaxed surface bonds, however, no significant distortion was observed. Also of note from these results is the increased relaxation going from the singly to doubly negative case and in the cluster with a fully relaxed surface. Given the energy differences observed in the cluster calculations with different surface conditions, we conclude that the contribution from these changes must be very slight. Comparing this with other theoretical work on the structure of the divacancy, we find that the distortions we observe are of the same type and similar magnitude to those observed by Coutinho *et al.*,¹⁵ Ögüt *et al.*¹⁰ have also published work on the divacancy structure in Ge, and their results show slightly larger distortions than are observed in either this study or the study of Coutinho *et al.*

IV. SUMMARY

The structures resulting from the calculations presented here show the similar JT distortion magnitudes to previous work by Coutinho *et al.*¹⁵ Following the conclusions of this previous study, we also find that the distortions are small, and the differences between the studies can be attributed to small differences in calculation parameters.

The supercell calculations showed that the vacancies are essentially free at fourth neighbor separation. Binding and migration energies of about 0.7 eV were found for the neutral and charged defects. Assuming a vacancy migration barrier of 0.2 eV gives a dissociation energy of V_2 to be about 0.9 eV. This dissociation energy is lower than the experimental estimate of 1.3 eV assuming this mechanism. Instead, the supercell results support the idea that V_2 anneals by diffusion as the 0.7 eV barrier found is reasonably close to the experimental estimate of 1.0 eV. However, band-structure calculations for supercells containing a divacancy showed that the energy levels introduced into the band gap by the divacancy crossed into the valance band for a range of \mathbf{k} points, including some used for sampling the Brillouin zone. As a result, the supercell calculations were viewed with some suspicion.

Migration barriers deduced from cluster calculations were found to be largely insensitive to surface conditions, yielding essentially the same results for clusters with strained or relaxed germanium-hydrogen bonds and with fully relaxed surfaces. Binding energies of both neutral and charged defects deduced from runs where the vacancies are separated at fourth neighbor were also insensitive to the method of relaxation. It appears that the proximity of the separated vacancies with the cluster surface causes an 0.2 eV overestimate of the binding energy of the vacancies in V_2 .

The dissociation energy found by the cluster method is the binding energy plus the migration energy of a single vacancy taken to be 0.2 eV. This gives about 1.5–1.7 eV once the

overestimation from the surface interactions is taken into account. This is to be compared with an experimental estimate of ~ 1.3 eV assuming that the defect anneals by dissociation. The migration energy of V_2 is found to be about 1.1 eV and very close to the experimental estimate of 1.0 eV assuming the same mechanism. Both the binding and migration energy barriers are shown to increase with increasingly negatively charged systems.

The charge dependence of the migration barrier of the divacancy is found to be opposite to that recently calculated for the single vacancy in germanium.¹ This trend in the divacancy case can be explained by considering the structure results above along with the migration path observed. The relaxations increase the energy of migration by reducing the space through which the mobile atom moves, thereby increasing the distortion required to allow it to pass. Increasing relaxation in more negative charge states further increases this barrier.

V. CONCLUSION

Calculations have been performed within the supercell and cluster methodologies to give the binding and migration energies of the divacancy in germanium in charge states ranging from the singly positive to the doubly negative. The standard MP-2³ \mathbf{k} -point sampling technique gave estimates of 0.7 and 0.9 eV for the migration and dissociation barriers. These values imply that as the defect becomes mobile, it will quickly dissociate and the loss mechanism must involve dissociation. However, in this case the calculated barrier is much lower than an experimental estimate of 1.3 eV based on an annealing temperature of 160 °C.^{16–18} These barriers are insensitive to charge state which has been attributed to a crossing of defect energy levels with the valance-band levels in Ge. This is a consequence of the very small band gap in Ge found in DFT calculations and reduces confidence in the results.

Using large H-terminated clusters give values of about 1.6 and 1.1 eV for the dissociation and migration barriers, respectively, and which are insensitive to surface conditions. These increase by ~ 0.1 eV for negative-charged divacancies. The cluster results show that the divacancy becomes mobile before dissociation and the calculated diffusion barrier is close to the experimental estimate of 1.0 eV based purely on a diffusion mechanism. Therefore, we expect most divacancies will anneal by diffusion provided the trap density is high enough.

ACKNOWLEDGMENTS

C.J. would like to thank A. Carvalho and J. Coutinho for helpful discussion and comments, and the EPSRC and INTAS (Grant No. 03-50-4529) for financial support.

*Electronic address: janke@excc.ex.ac.uk

- ¹H. M. Pinto, J. Coutinho, V. J. B. Torres, S. Öberg, and P. R. Briddon, *Mater. Sci. Semicond. Process.* **9**, 498 (2006).
- ²A. Fazio, A. Janotti, A. J. R. da Silva, and R. Mota, *Phys. Rev. B* **61**, R2401 (2000).
- ³A. Polity and F. Rudolf, *Phys. Rev. B* **59**, 10025 (1999).
- ⁴R. E. Whan, *Appl. Phys. Lett.* **6**, 221 (1965).
- ⁵A. J. R. da Silva, R. Baierle, R. Mota, and A. Fazio, *Physica B* **302**, 364 (2001).
- ⁶H. Haesslein, R. Sielemann, and C. Zistl, *Phys. Rev. Lett.* **80**, 2626 (1998).
- ⁷J. Coutinho, R. Jones, V. J. B. Torres, M. Barroso, S. Öberg, and P. R. Briddon, *J. Phys.: Condens. Matter* **17**, L521 (2005).
- ⁸F. C. Gozzo, M. N. Eberlin, and I. Chambouleyron, *J. Non-Cryst. Solids* **299**, 174 (2002).
- ⁹A. Janotti, R. Baierle, A. J. R. da Silva, R. Mota, and A. Fazio, *Physica B* **273**, 575 (1999).
- ¹⁰S. Ögüt and J. R. Chelikowsky, *Phys. Rev. B* **64**, 245206 (2001).
- ¹¹M. Werner, H. Mehrer, and H. D. Hochheimer, *Phys. Rev. B* **32**, 3930 (1985).
- ¹²H. Bracht, N. A. Stolwijk, and H. Mehrer, *Phys. Rev. B* **43**, 14465 (1991).
- ¹³D. Poelman, O. De Gryse, N. De Roo, O. Janssens, P. Clauws, W. Bras, I. D. Dolbnya, and I. Romandic, *J. Appl. Phys.* **96**, 6164 (2004).
- ¹⁴S. Hens, J. Vanhellemont, D. Poelman, P. Clauws, I. Romandic, A. Theuwis, F. Holsteys, and J. Van Steenberg, *Appl. Phys. Lett.* **87**, 061915 (2005).
- ¹⁵J. Coutinho, V. J. B. Torres, R. Jones, A. Carvalho, S. Öberg, and P. R. Briddon, *Appl. Phys. Lett.* **88**, 091919 (2006).
- ¹⁶F. Poulin and J. C. Bourgoin, *Rev. Phys. Appl.* **15**, 15 (1980).
- ¹⁷P. M. Mooney, F. Poulin, and J. C. Bourgoin, *Phys. Rev. B* **28**, 3372 (1983).
- ¹⁸J. Fage-Pedersen, A. N. Larsen, and A. Mesli, *Phys. Rev. B* **62**, 10116 (2000).
- ¹⁹J. E. Whitehouse, *Radiation Damage and Defects in Semiconductors* (London Institute of Physics, London, 1973).
- ²⁰S. R. Morrison and R. C. Newman, *J. Phys. C* **6**, 1973 (1981).
- ²¹G. D. Watkins and J. W. Corbett, *Phys. Rev.* **138**, 543 (1965).
- ²²R. Jones, A. Carvalho, J. Coutinho, V. J. B. Torres, S. Öberg, and P. R. Briddon, *Solid State Phenom.* **108–109**, 697 (2005).
- ²³P. R. Briddon and R. Jones, *Phys. Status Solidi B* **217**, 131 (2000).
- ²⁴S. Goedecker, M. Teter, and J. Hutter, *Phys. Rev. B* **54**, 1703 (1996).
- ²⁵J. P. Perdew and Y. Wang, *Phys. Rev. B* **45**, 13244 (1992).
- ²⁶C. Hartwigsen, S. Goedecker, and J. Hutter, *Phys. Rev. B* **58**, 3641 (1998).
- ²⁷H. J. Monkhorst and J. D. Pack, *Phys. Rev. B* **13**, 5188 (1976).
- ²⁸*CRC Handbook of Chemistry and Physics*, 81st ed., edited by D. R. Lide (CRC, Boca Raton, FL, 2000).
- ²⁹G. S. Hwang and William A. Goodard III, *Phys. Rev. B* **65**, 233205 (2002).
- ³⁰G. Henkelman and H. Jónsson, *J. Chem. Phys.* **113**, 9978 (2000).
- ³¹A. Carvalho, R. Jones, V. J. B. Torres, S. Öberg, J. M. Campanera Alsina, M. Shaw, and P. R. Briddon (unpublished).
- ³²J. Coutinho, S. Öberg, V. J. B. Torres, M. Barroso, R. Jones, and P. R. Briddon, *Phys. Rev. B* **73**, 235213 (2006).
- ³³J. Coutinho, R. Jones, P. R. Briddon, and S. Öberg, *Phys. Rev. B* **62**, 10824 (2000).